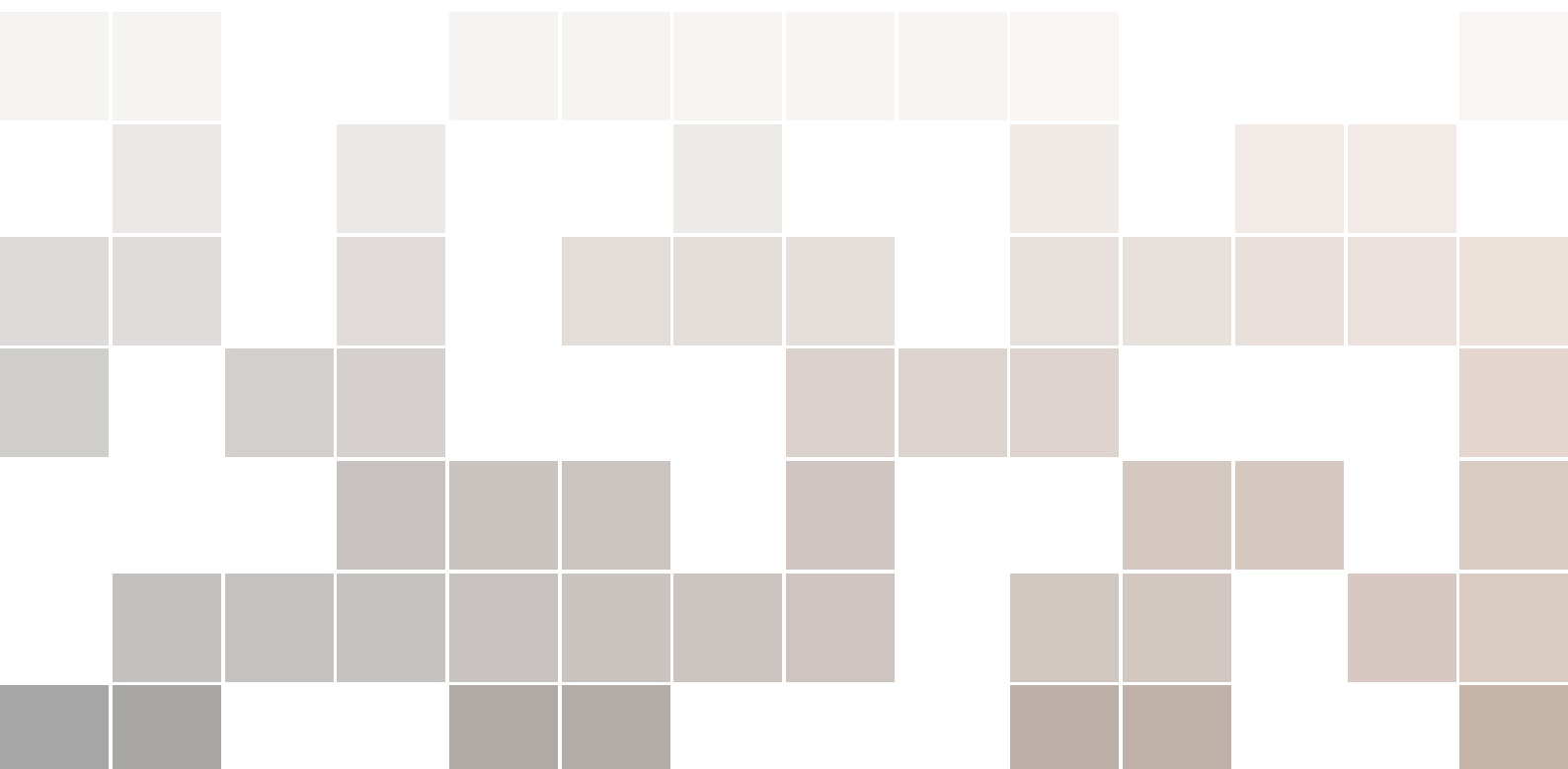


# Krittika Summer Projects 2023

Solar System Dynamics

Ramesh Dange





# Contents

<b>1</b>	<b>Theory</b> .....	<b>5</b>
1.1	Newtonian Gravity	5
1.2	Two Body Problem	5
1.3	Reduced Three Body Problem	5
1.3.1	Lagrangian Points .....	6
1.3.2	Virial Theorem .....	6
1.4	Photon Path Around Non Rotating Blackhole	6
1.5	Analemma	6
1.6	Integrators	7
1.6.1	Euler Method .....	7
1.6.2	Euler-Richardson Method .....	7
	8subsection.1.6.3	
<b>2</b>	<b>Implementation (Foundation)</b> .....	<b>9</b>
2.1	Introduction	9
2.2	Establishing Core C++ Classes	9
<b>3</b>	<b>Two Body system</b> .....	<b>11</b>
3.1	Inroduction	11
3.2	Circular Trajectories	11
3.3	Elliptic Trajectories	11
3.4	Hyperbolic Trajectories	12
3.5	Plots	12

<b>4</b>	<b>Restricted Three Body System</b> .....	<b>15</b>
4.1	Problem Setup	15
4.2	Contour Plot of Potential in the Rotating Frame	15
4.3	Tadpole and Horseshoe Orbits	15
4.3.1	Tadpole Orbits .....	16
4.3.2	Horseshoe Orbits .....	16
4.4	Plots	16
<b>5</b>	<b>Photons around a Non-Rotating Black Hole</b> .....	<b>19</b>
5.1	Problem Setup	19
5.2	Initial Conditions	19
5.2.1	Trajectory 1 .....	19
5.2.2	Trajectory 2 .....	19
5.3	Plots	20
<b>6</b>	<b>Analemma</b> .....	<b>21</b>
6.1	Problem Setup	21
6.2	Initial Conditions	21
6.2.1	Planet Earth .....	21
6.2.2	Planet Mar .....	21
6.3	Plots	22
<b>7</b>	<b>Kirkwood Gaps</b> .....	<b>25</b>
7.1	Problem Setup	25
7.2	Initial Conditions	25
7.3	Plots	26
7.4	Conclusion	26



# 1. Theory

## 1.1 Newtonian Gravity

Newtonian gravity, formulated by Sir Isaac Newton, describes the force of attraction between two objects with mass. According to Newton's law of universal gravitation, the gravitational force between two objects is directly proportional to the product of their masses and inversely proportional to the square of the distance between them.

$$G \frac{m_1 \cdot m_2}{r^2} \quad (1.1)$$

## 1.2 Two Body Problem

The Two-Body Problem involves the study of the motion of two celestial bodies under the influence of their mutual gravitational attraction. This problem assumes that the mass of each body is concentrated at its center of mass and neglects the gravitational effects of other celestial bodies.

The motion of the two bodies can be described by solving the equations of motion derived from Newton's law of universal gravitation. The solutions can yield various orbital shapes, including circular, elliptical, parabolic, and hyperbolic orbits.

## 1.3 Reduced Three Body Problem

The Reduced 3-Body Problem is a simplified version of the gravitational interaction between three celestial bodies, where one body is significantly less massive than the other two. The motion of the lighter body can be approximated by considering the gravitational forces exerted by the two more massive bodies.

By applying the principle of barycenter, the system can be transformed into a Two-Body Problem. The reduced mass ( $\mu$ ) is defined as:

$$\mu = \frac{m_1 \cdot m_2}{m_1 + m_2} \quad (1.2)$$

### 1.3.1 Lagrangian Points

Lagrangian points, named after Joseph-Louis Lagrange, are five points in a Two-Body System where the gravitational forces and centrifugal forces balance each other, allowing for stable positions for other smaller bodies. These points are denoted as  $L1$ ,  $L2$ ,  $L3$ ,  $L4$ , and  $L5$ .

Lagrangian points can be determined by solving the equations of motion for a small mass located at a Lagrangian point, where the gravitational force from the two primary masses and the centrifugal force are in equilibrium.

### 1.3.2 Virial Theorem

The Virial theorem is a mathematical relationship that relates the average kinetic energy ( $K$ ) to the average potential energy ( $U$ ) of a system in equilibrium. It states that for a stable system, the average kinetic energy is equal to minus half the average potential energy:

$$2K = -U \quad (1.3)$$

## 1.4 Photon Path Around Non Rotating Blackhole

The Schwarzschild radius of a black hole is given by

$$r_{\text{BH}} = \frac{2GM_{\text{BH}}}{c^2}, \quad (1.4)$$

where  $M_{\text{BH}}$  represents the mass of the black hole. The Schwarzschild radius defines the radius at which the escape velocity equals the speed of light, delineating the point of no return for any object within this boundary.

To plot the trajectory of a photon around a non-rotating black hole, we will utilize the energy and angular momentum conservation equations:

$$\frac{1}{2}\dot{r}^2 + \frac{l^2}{2r^2} - \frac{l^2 r_{\text{BH}}}{2r^3} = E \quad (\text{for energy}), \quad (1.5)$$

and

$$r^2 \dot{\theta} = l \quad (\text{for angular momentum}), \quad (1.6)$$

where  $\dot{r}$  represents the derivative of  $r$  with respect to time,  $\theta$  is the angular coordinate,  $l$  is the specific angular momentum of the photon,  $E$  is the energy of the photon, and  $c$  is the speed of light.

## 1.5 Analemma

An analemma is a graphical representation of the Sun's apparent motion in the sky over the course of a year, as observed from a fixed location on Earth at the same time each day. This trajectory is shaped by the combination of the Earth's axial tilt and its elliptical orbit around the Sun.

The rate of change of the angle  $\theta$  with respect to time  $t$  is given by the equation:

$$\frac{d\theta}{dt} = \frac{(1 + e \cos \theta)^2}{T \cdot (1 - e^2)^{1.5}} \quad (1.7)$$

Here,  $\theta$  represents the current position of the planet from its perihelion,  $e$  is the eccentricity of the planet's orbit, and  $T$  denotes the period of the planet's orbital motion.

The declination  $\delta$  is calculated using the equation:

$$\delta = \sin^{-1}(\sin \varepsilon \cdot \sin \lambda) \quad (1.8)$$

In this equation,  $\varepsilon$  represents the axial tilt of the planet, and  $\lambda$  corresponds to the geocentric ecliptic longitude of the stellar object in question.

The right ascension  $\alpha$  is calculated using the equation:

$$\cos \alpha = \frac{\cos \lambda}{\cos \delta} \quad (1.9)$$

In this equation,  $\lambda$  represents the geocentric ecliptic longitude of the stellar object, and  $\delta$  is the declination.

The altitude  $a$  (at the north pole) is calculated using the below equation:

$$a = \delta \quad (1.10)$$

The azimuth  $A$  (at the north pole) is calculated using the equation:

$$A = \alpha - \omega \cdot t \quad (1.11)$$

In these equations,  $\delta$  represents the declination,  $\alpha$  represents the right ascension,  $\omega$  denotes the angular velocity of revolution, and  $t$  represents the time.

## 1.6 Integrators

The accurate numerical solution of differential equations plays a crucial role in various scientific and engineering applications. Integrators, or numerical integration methods, are essential tools used to approximate the solutions of ordinary differential equations (ODEs).

### 1.6.1 Euler Method

The Euler method is a simple numerical integration technique used to approximate the solution of ordinary differential equations (ODEs). It is based on the idea of approximating the derivative of a function using a finite difference. The basic algorithm of the Euler method is as follows:

- Given an initial condition  $y_0$  at  $t = t_0$ .
- Choose a step size  $h$ .
- Iterate using the following formula:
  - Calculate the derivative  $f(t_n, y_n)$  at each time step.
  - Update the solution using the formula  $y_{n+1} = y_n + h \cdot f(t_n, y_n)$ .
  - Update the time  $t_n = t_0 + n \cdot h$ .

The Euler method is relatively straightforward to implement but may introduce significant errors, particularly for large step sizes or highly nonlinear systems. It is considered a first-order numerical integration method.

### 1.6.2 Euler-Richardson Method

The Euler-Richardson method, also known as the semi-implicit Euler method or the modified Euler method, is an improvement over the basic Euler method. It provides better accuracy by considering a midpoint approximation for the derivative. The algorithm for the Euler-Richardson method is as follows:

- Given an initial condition  $y_0$  at  $t = t_0$ .
- Choose a step size  $h$ .
- Iterate using the following formula:
  - Calculate the derivative  $f(t_n, y_n)$  at each time step.
  - Update the solution using the formula  $y_{n+1} = y_n + h \cdot f(t_n + \frac{h}{2}, y_n + \frac{h}{2} \cdot f(t_n, y_n))$ .
  - Update the time  $t_n = t_0 + n \cdot h$ .

The Euler-Richardson method considers the derivative at a midpoint, resulting in improved accuracy compared to the basic Euler method. However, it still has limitations for highly nonlinear systems or large step sizes.

### 1.6.3 Runge-Kutta (RK4) Method<sup>1</sup>

The Runge-Kutta (RK4) method is a widely used numerical integration technique for solving ordinary differential equations (ODEs). It offers higher accuracy compared to the Euler methods by utilizing multiple evaluations of the derivative at various points within a time step. The RK4 method employs a fourth-order approximation, resulting in improved accuracy for a wide range of systems. The algorithm for the RK4 method is as follows:

$$k_1 = f(x_n, t_n) \cdot \Delta t \quad (1.12)$$

$$k_2 = f\left(x_n + \frac{k_1}{2}, t_n + \frac{\Delta t}{2}\right) \cdot \Delta t \quad (1.13)$$

$$k_3 = f\left(x_n + \frac{k_2}{2}, t_n + \frac{\Delta t}{2}\right) \cdot \Delta t \quad (1.14)$$

$$k_4 = f(x_n + k_3, t_n + \Delta t) \cdot \Delta t \quad (1.15)$$

$$x_{n+1} = x_n + \frac{1}{6}(k_1 + 2k_2 + 2k_3 + k_4) \quad (1.16)$$

The application of the fourth-order Runge-Kutta algorithm to Newton's equation of motion yields the following update equations:

$$k_{1v} = a(x_n, v_n, t_n) \cdot \Delta t \quad (1.17)$$

$$k_{1x} = v_n \cdot \Delta t \quad (1.18)$$

$$k_{2v} = a\left(x_n + \frac{k_{1x}}{2}, v_n + \frac{k_{1v}}{2}, t_n + \frac{\Delta t}{2}\right) \cdot \Delta t \quad (1.19)$$

$$k_{2x} = \left(v_n + \frac{k_{1v}}{2}\right) \cdot \Delta t \quad (1.20)$$

$$k_{3v} = a\left(x_n + \frac{k_{2x}}{2}, v_n + \frac{k_{2v}}{2}, t_n + \frac{\Delta t}{2}\right) \cdot \Delta t \quad (1.21)$$

$$k_{3x} = \left(v_n + \frac{k_{2v}}{2}\right) \cdot \Delta t \quad (1.22)$$

$$k_{4v} = a(x_n + k_{3x}, v_n + k_{3v}, t_n + \Delta t) \cdot \Delta t \quad (1.23)$$

$$k_{4x} = (v_n + k_{3v}) \cdot \Delta t \quad (1.24)$$

And the updated values of velocity ( $v_{n+1}$ ) and position ( $x_{n+1}$ ) for the next time step are given by:

$$v_{n+1} = v_n + \frac{1}{6}(k_{1v} + 2k_{2v} + 2k_{3v} + k_{4v}) \quad (1.25)$$

$$x_{n+1} = x_n + \frac{1}{6}(k_{1x} + 2k_{2x} + 2k_{3x} + k_{4x}) \quad (1.26)$$

<sup>1</sup>Gould, H., Tobochnik, J., Christian, W. (2016). An Introduction to Computer Simulation Methods Applications to Physical System. Addison-Wesley Publishing Company. Appendix 3A.





## 2. Implementation (Foundation)

### 2.1 Introduction

The implementation of complex systems often requires a combination of programming languages to optimize performance and flexibility. This chapter presents the foundational implementation for our simulation, utilizing C++ as the underlying language and Python for plotting and analysis. This approach harnesses the high-performance capabilities of C++ for the simulation core, while leveraging the user-friendly interface and extensive libraries of Python for analysis and visualization.

### 2.2 Establishing Core C++ Classes

The establishment of the implementation framework commences with the design and implementation of two core classes: "phyvec" and "body." The "phyvec" class is responsible for representing vectors utilized in the simulation, furnishing essential functionalities for performing vector-related operations and computations. Conversely, the "body" class assumes a pivotal role in simulating individual entities within the system. This class encapsulates the intrinsic attributes and behaviors of these entities, facilitating the modeling of their dynamic properties and interactions. Additionally, a distinct file is devised to contain integrators. Furthermore, an abstract base class denoted as "System" is introduced, incorporating polymorphic behavior. This base class serves as the foundation for deriving numerous other classes within the system architecture.





## 3. Two Body system

### 3.1 Introduction

This chapter explores the simulation and analysis of two-body systems, investigating various initial conditions and examining the resulting trajectories.

### 3.2 Circular Trajectories

Circular orbits are characterized by a constant radius, where the gravitational force acting between the two bodies is balanced by the centripetal force. The initial conditions play a crucial role in achieving circular trajectories. By setting equal masses for both bodies and providing appropriate tangential velocities, circular orbits can be simulated. The following initial conditions are considered for circular trajectories:

Body 1:

Mass:  $1 \times 10^{21}$  Position: (0.0,0.0,0.0) Velocity: (0.0,1724.0033713806993,0.0)

Body 2:

Mass:  $1 \times 10^{21}$  Position: (32336.42425758127,0.0,0.0) Velocity: (0.0,-1149.3355809204663,0.0)

### 3.3 Elliptic Trajectories

Elliptical orbits represent a common type of motion in the two-body system. These trajectories exhibit non-zero eccentricity, which determines the shape and orientation of the elliptical path. By adjusting the initial conditions, such as varying the eccentricity and semi-major axis, a range of elliptical trajectories can be obtained. The following initial conditions are considered for elliptical trajectories:

Body 1:

Mass:  $1 \times 10^{21}$  Position: (0.0,0.0,0.0) Velocity: (0.0,1005.668633305408,0.0)

Body 2:

Mass:  $1 \times 10^{21}$  Position: (32336.42425758127,0.0,0.0) Velocity: (0.0,-1149.3355809204663,0.0)

### 3.4 Hyperbolic Trajectories

Hyperbolic orbits occur when the bodies possess sufficient energy to overcome each other's gravitational attraction. In these trajectories, the bodies move along hyperbolas, with the distance between them continually increasing. By manipulating the initial conditions, such as increasing the relative velocity or altering the impact parameter, hyperbolic trajectories can be simulated. The following initial conditions are considered for hyperbolic trajectories:

Body 1:

Mass:  $1 \times 10^{21}$  Position: (0.0,0.0,0.0) Velocity: (0.0,3160.672847531282,0.0)

Body 2:

Mass:  $1 \times 10^{21}$  Position: (32336.42425758127,0.0,0.0) Velocity: (0.0, -1149.3355809204663,0.0)

### 3.5 Plots

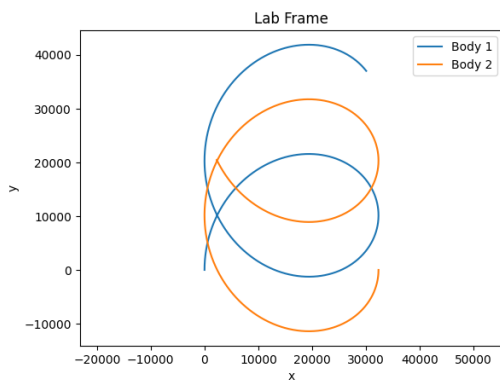


Figure 3.1: Lab Frame - Euler Method

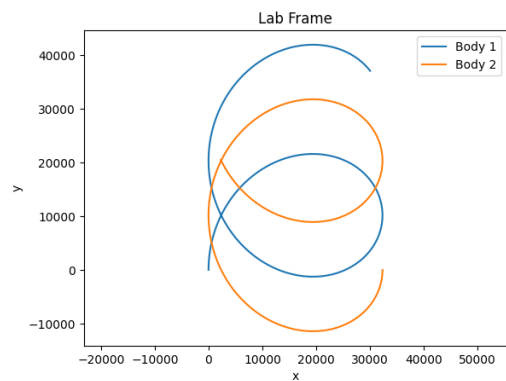


Figure 3.2: Lab Frame - Euler-Richardson Method

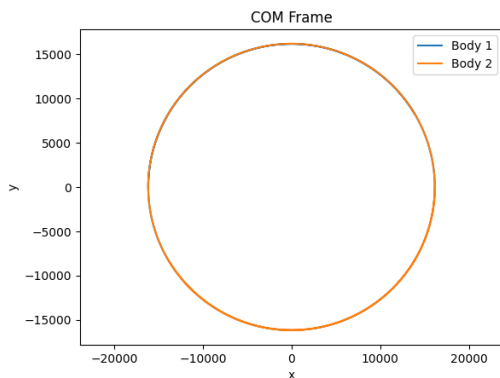


Figure 3.3: COM Frame - Euler Method

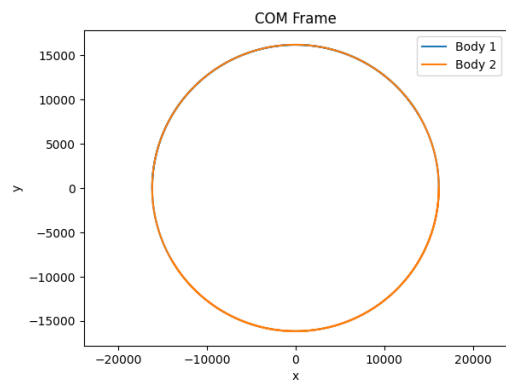


Figure 3.4: COM Frame - Euler-Richardson Method

Figure 3.5: Plots of the two-body system in different frames using the Euler method and Euler-Richardson method. The top row shows the plots in the lab frame, while the bottom row shows the plots of circular trajectories in the center of mass (COM) frame. The left column corresponds to the Euler method, and the right column corresponds to the Euler-Richardson method.

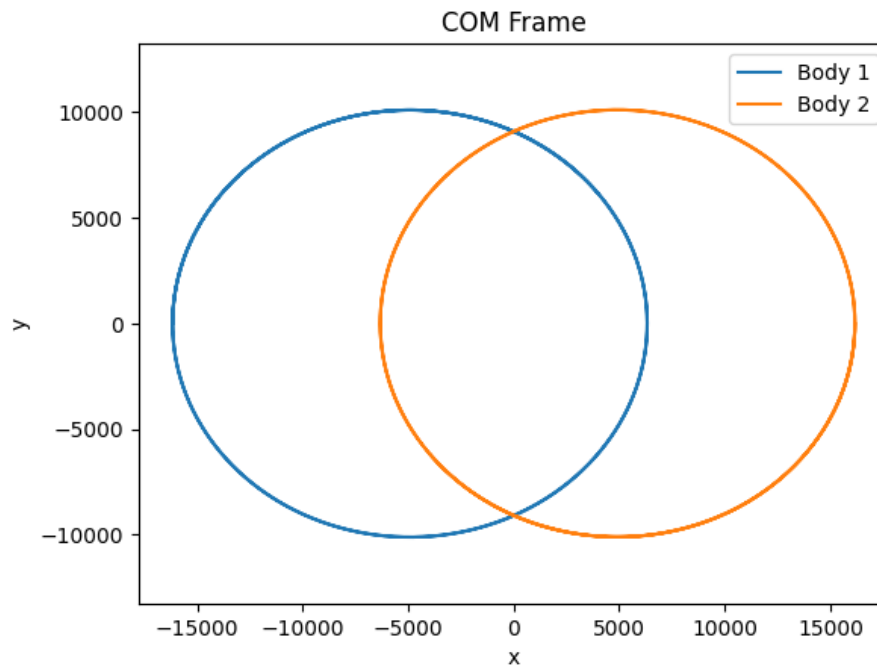


Figure 3.6: Elliptic trajectory in the center of mass (COM) frame using the forward Euler method.

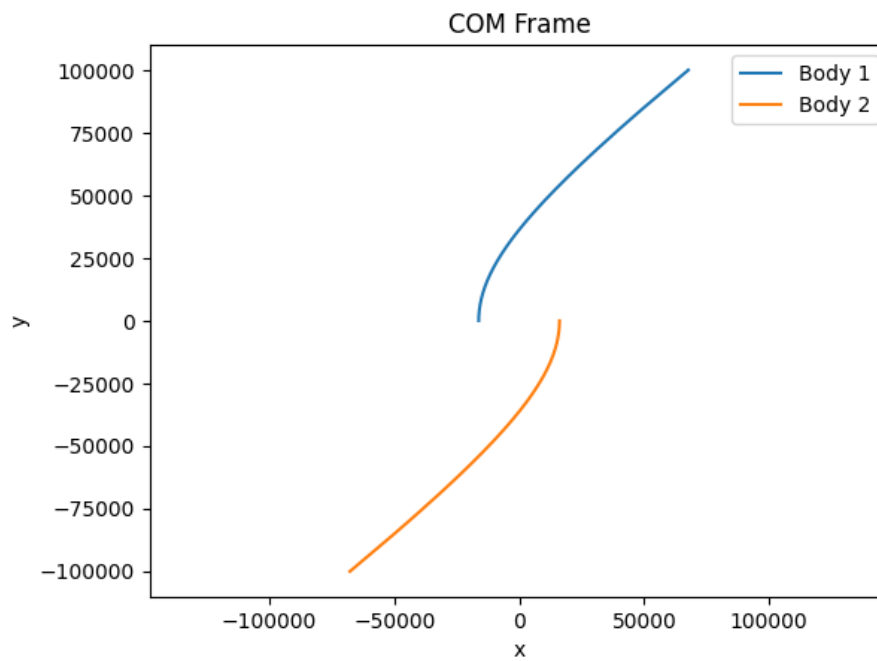


Figure 3.7: Hyperbolic trajectory in the center of mass (COM) frame using the forward Euler method.







## 4. Restricted Three Body System

The restricted three-body system is a celestial mechanics problem that involves the interaction of three celestial bodies, where one body is significantly smaller in mass compared to the other two. In this chapter, we explore the dynamics of the restricted three-body system and analyze the behavior of the third body in the rotating frame.

### 4.1 Problem Setup

The restricted three-body system consists of two primary bodies, referred to as the primary body 1 and primary body 2, and a third body of much smaller mass. The primary bodies exert gravitational forces on each other, while the third body is influenced by the gravitational fields of the primary bodies.

To study the dynamics of the system, we consider the system in a rotating frame of reference. In this frame, the two primary bodies are fixed, and the coordinate system rotates with a constant angular velocity equal to the average angular velocity of the two primary bodies.

### 4.2 Contour Plot of Potential in the Rotating Frame

One way to analyze the behavior of the third body in the restricted three-body system is by examining the potential energy landscape in the rotating frame. The potential energy represents the gravitational potential experienced by the third body due to the presence of the two primary bodies.

The two primary bodies in the restricted three-body system have the following masses:

Primary Body 1: Mass:  $1 \times 10^{21}$

Primary Body 2: Mass:  $3 \times 10^{21}$

Distance between the two primary bodies: 32000

### 4.3 Tadpole and Horseshoe Orbits

In celestial mechanics, certain regions within a restricted three-body system exhibit fascinating orbital behaviors known as horseshoe and tadpole orbits.

### 4.3.1 Tadpole Orbits

Tadpole orbits are similar to horseshoe orbits but occur around the L4 and L5 Lagrangian points. In these orbits, the gravitational forces of the primary bodies create stable equilibrium points at the L4 and L5 points, where the centrifugal force and gravitational forces balance. A smaller body placed near these points exhibits a tadpole-shaped orbit, with the head of the tadpole corresponding to the Lagrangian point and the tail extending along the orbit. The following initial conditions are considered for tadpole orbits (in lab frame):

Body 1:

Mass:  $1.4968355 \times 10^{10}$

Position: (0.0, 0.0, 0.0)

Velocity:  $(0.0, -3.162277660168379 \times 10^{-2}, 0.0)$

Body 2:

Mass:  $1.49833 \times 10^7$

Position: (1.0, 0.0, 0.0)

Velocity:  $(0.0, 9.994998749374610 \times 10^{-01}, 0.0)$

Body 3:

Mass: 0.0

Position:  $(5.065000000000000 \times 10^{-01}, 8.725254037844385 \times 10^{-01}, 0.0)$

Velocity:  $(-8.725254037844385 \times 10^{-01}, 4.749083460498553 \times 10^{-01}, 0.0)$

### 4.3.2 Horseshoe Orbits

Horseshoe orbits occur when a smaller body appears to "hover" around the L3 Lagrangian point of the larger primary body. In this configuration, the gravitational forces of both primary bodies contribute to the motion of the smaller body, causing it to move in a horseshoe-shaped path with respect to the larger primary body. As the smaller body approaches the larger one, gravitational forces decelerate it, causing it to shift to the other side. This results in a repetitive motion resembling a horseshoe. The following initial conditions are considered for tadpole orbits (in lab frame):

Body 1:

Mass:  $1.4969046 \times 10^{10}$

Position: (0.0, 0.0, 0.0)

Velocity:  $(0.0, -0.030884867, 0.0)$

Body 2:

Mass:  $1.42922e \times 10^7$

Position: (1.0, 0.0, 0.0)

Velocity:  $(0.0, 0.99952295, 0.0)$

Body 3:

Mass: 0.0

Position:  $(-1.02745, 0.0, 0.0)$

Velocity:  $(0.0, -1.017985861589397, 0.0)$

## 4.4 Plots



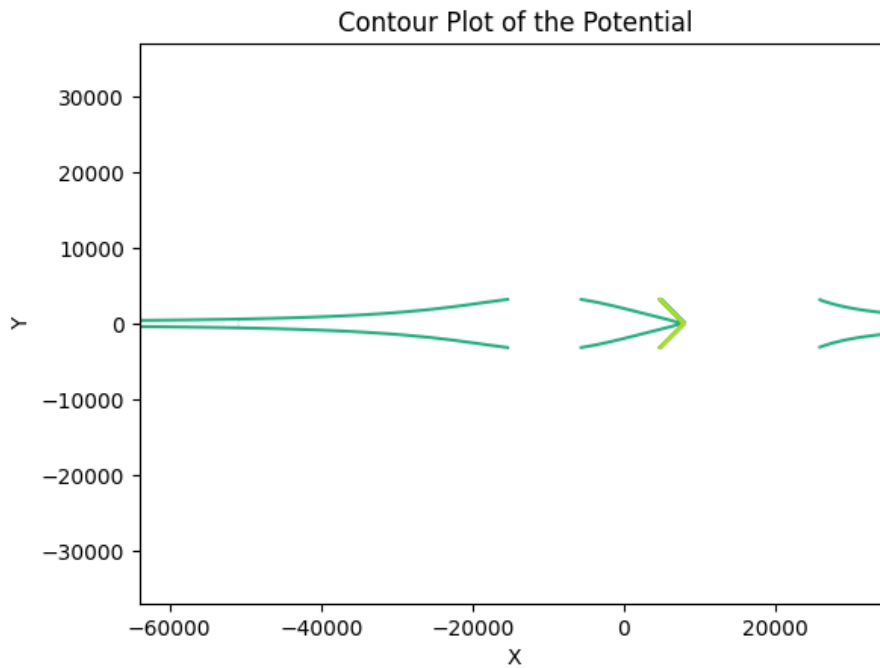


Figure 4.1: Contour plot of potential energy in the rotating frame for the restricted three-body system. The origin of the rotating frame is at the COM of the two bodies

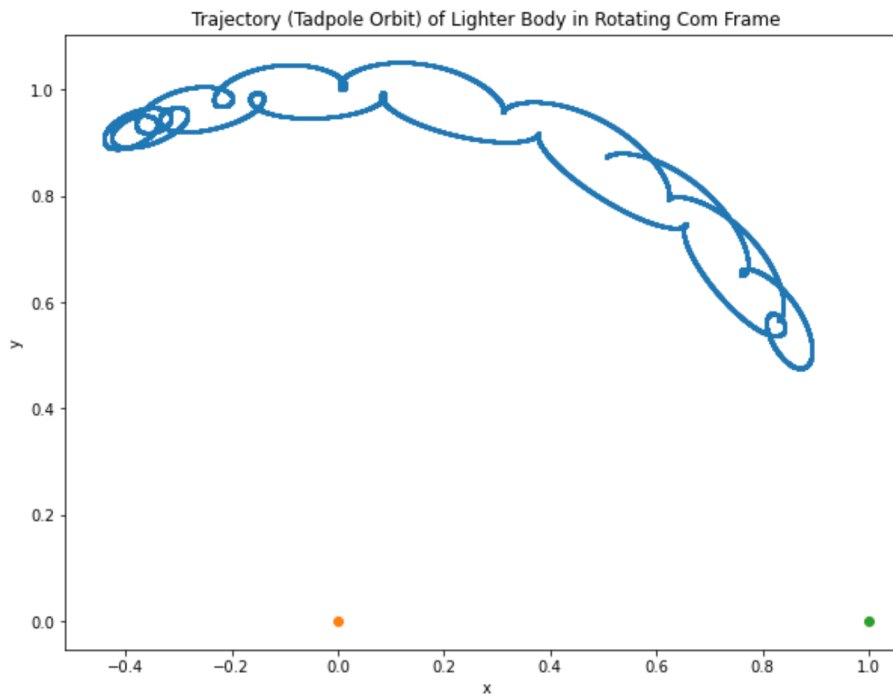


Figure 4.2: Tadpole orbit in the rotating COM frame

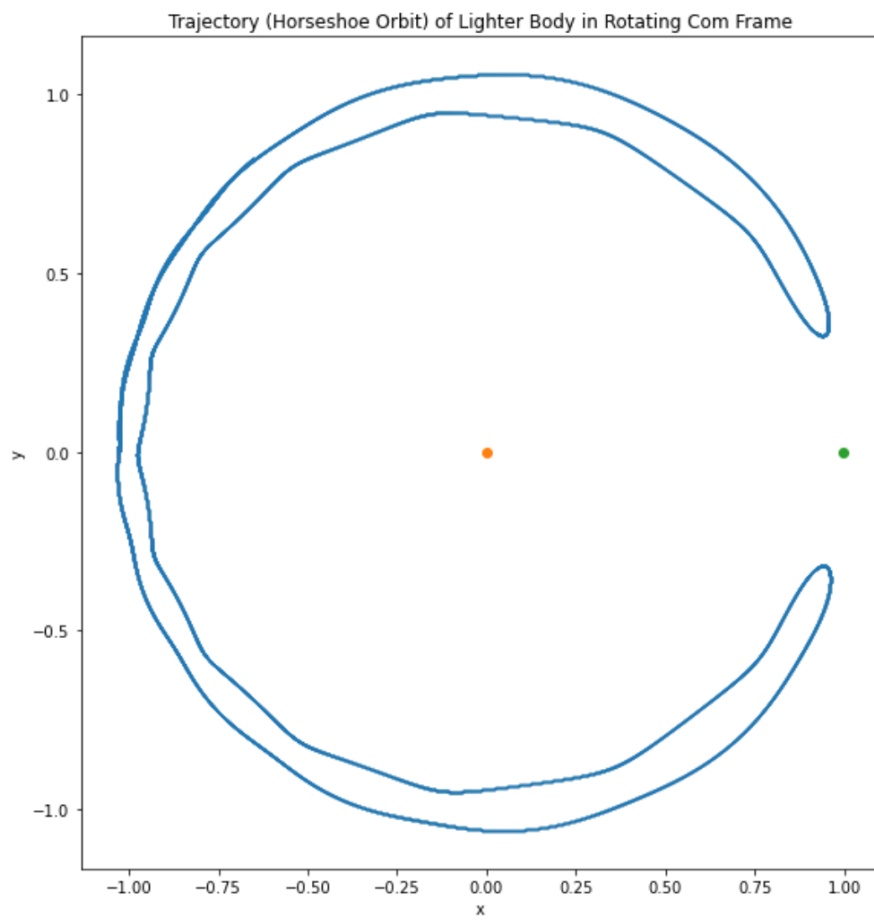


Figure 4.3: Horseshoe orbit in the rotating COM frame



## 5. Photons around a Non-Rotating Black Hole

In this chapter, we explore the captivating trajectory of a photon as it orbits a non-rotating black hole. The immense gravitational influence of the black hole affects the path of the photon, leading to fascinating observations.

### 5.1 Problem Setup

We consider a photon emitted from a distant source, traveling towards a non-rotating black hole. As the photon approaches the black hole, it follows a curved path due to the gravitational field. The goal is to analyze this trajectory and understand how factors such as the photon's initial velocity and distance from the black hole affect its path.

### 5.2 Initial Conditions

Speed of light: 200

Black Hole:

Mass:  $5.993335411022942 \times 10^{14}$

Position (of centre): (0.0, 0.0, 0.0)

Velocity (of centre): 0.0, 0.0, 0.0

#### 5.2.1 Trajectory 1

Photon:

Position: (5.0, 0.0, 0.0)

Velocity: (0.0,  $2.0 \times 10^{02}$ , 0.0)

#### 5.2.2 Trajectory 2

Photon:

Position: (5.0, 0.0, 0.0)

Velocity: ( $-1.0 \times 10^{02}$ ,  $1.732050807568877 \times 10^{02}$ , 0.0)

### 5.3 Plots

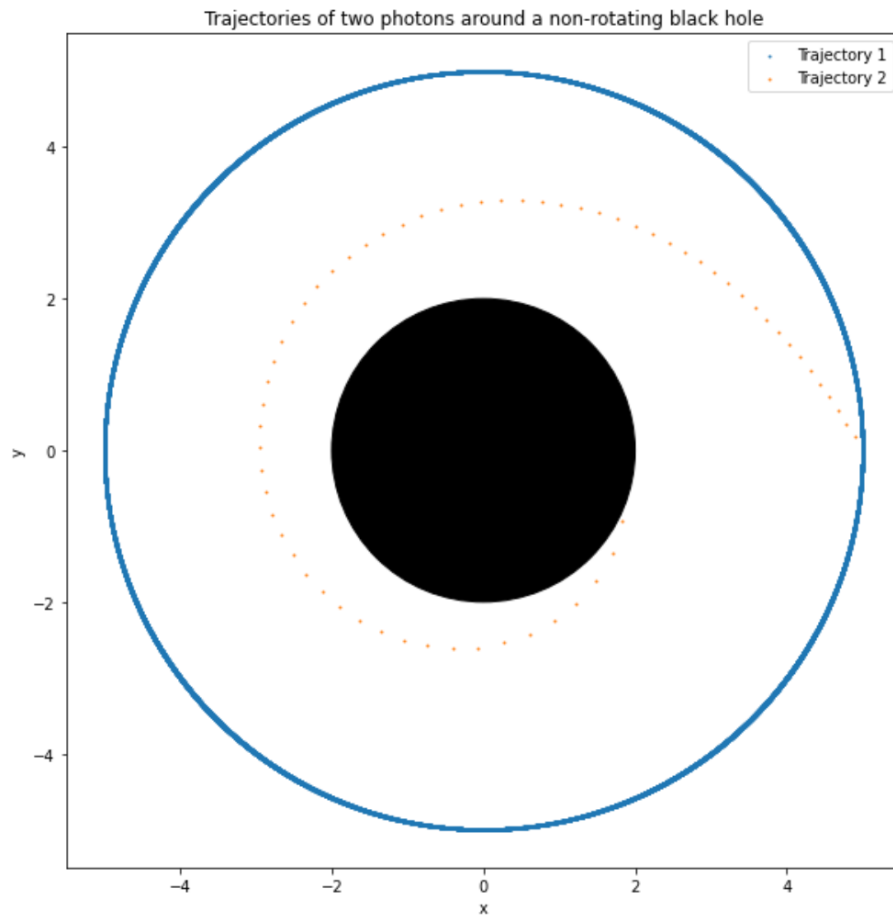


Figure 5.1: Trajectories of photons around a non-rotating black hole



## 6. Analemma

Through the analysis of the analemma, we gain a nuanced understanding of the complex interrelation between the Earth's axial tilt and its orbital eccentricity. These fundamental astronomical parameters converge to give rise to the distinctive figure-eight trajectory that charts the Sun's apparent motion throughout the year.

### 6.1 Problem Setup

In our study of the analemma, we consider the apparent motion of the Sun as observed from a fixed location on a planet's north pole.

### 6.2 Initial Conditions

#### 6.2.1 Planet Earth

Semi major axis:  $1.495978707 \times 10^{11}$   
Eccentricity : 0.0167  
Time period of revolution: 31557600  
Axial Tilt: 0.40910518  
Angular position of spring equinox ( $\theta_0$ ): 1.3089969  
Angle of current position from perihelion: 1.3089969

#### 6.2.2 Planet Mar

Semi major axis:  $2.27956 \times 10^{11}$   
Eccentricity : 0.0935  
Time period of revolution: 59356800  
Axial Tilt: 0.43964844  
Angular position of spring equinox ( $\theta_0$ ): 0.5  
Angle of current position from perihelion: 0.5  
(This is a fictitious planet. Everything except position of spring equinox are Mars' conditions, hence the fictitious name Mar)

### 6.3 Plots

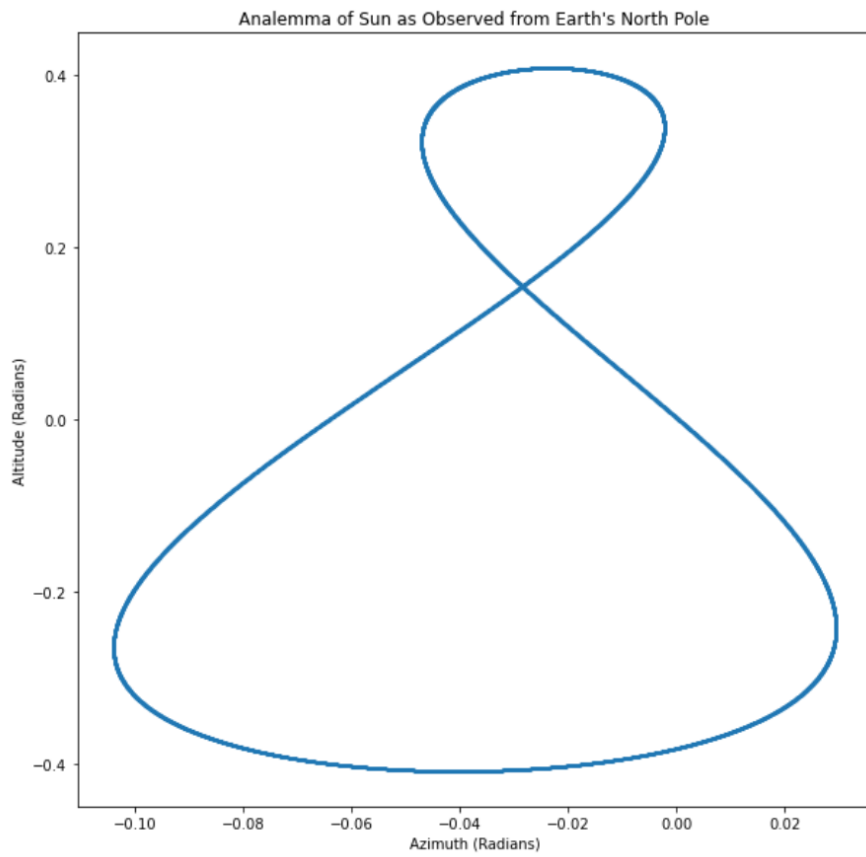


Figure 6.1: Analemma of Sun as Observed from Earth's North Pole

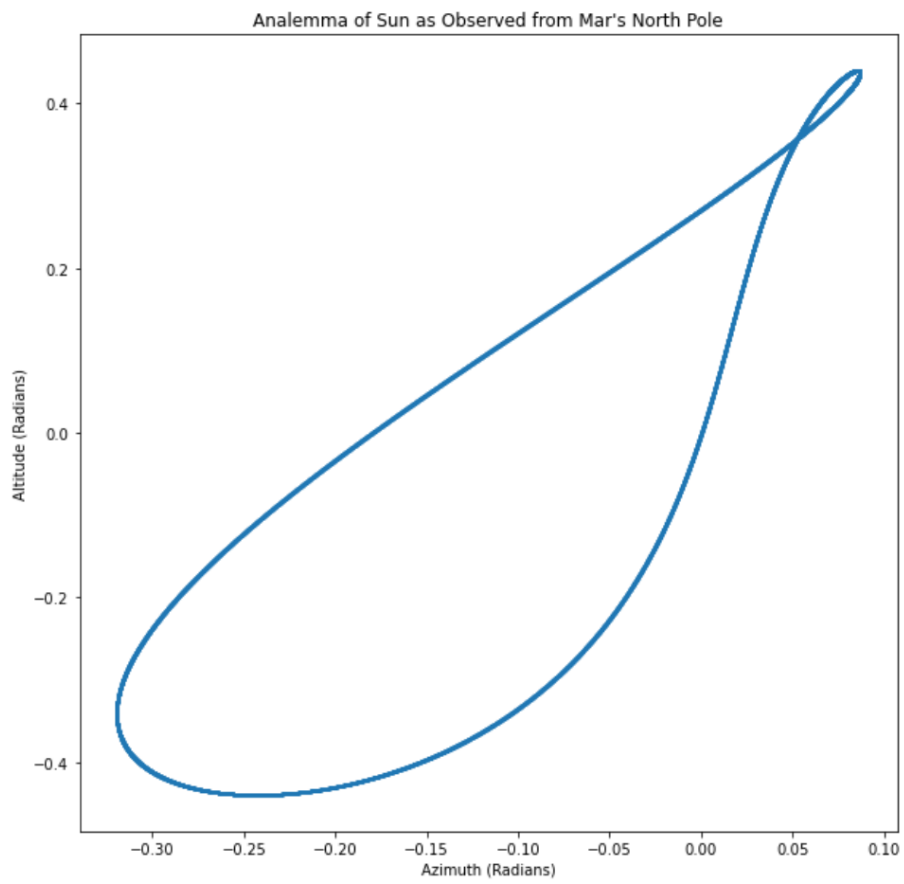


Figure 6.2: Analemma of Sun as Observed from Mar's North Pole





## 7. Kirkwood Gaps

Kirkwood gaps are regions in the asteroid belt that are depleted of asteroids due to the gravitational influence of Jupiter. These gaps occur at specific distances from the Sun, where the orbital period of an asteroid is a simple fraction of Jupiter's orbital period.

The gravitational influence of Jupiter causes asteroids in these gaps to experience a periodic force. This force can perturb the asteroids' orbits, causing them to be ejected from the belt or to be moved to other parts of the belt. As a result, these gaps are almost empty of asteroids.

### 7.1 Problem Setup

To simulate Kirkwood gaps, We will treat the Sun and Jupiter as massive bodies and asteroids as light bodies. The orbital of Jupiter can be approximated as a circle. Because of their light mass, the asteroids' interaction among themselves can be neglected. Thus, each asteroid, Sun, and Jupiter form an independent Circular Restricted Three Body Problem. The problem of finding Kirkwood gaps is thus reduced to several independent Circular Restricted Three Body Problems.

### 7.2 Initial Conditions

Sun: Mass: 1

Position: (0.0,0.0,0.0)

Velocity: (0.0,  $-2.696559482990327 \times 10^{-09}$ , 0.0)

Jupiter: Mass:  $3.774374561100000 \times 10^{-03}$

Position: (5.203812938610000, 0.0, 0.0)

Velocity: (0.0,  $4.389221587670570 \times 10^{-08}$ , 0.0)

Asteroids:

Mass: 0

Position: Both  $r$  and  $\theta$  are chosen randomly such that  $r$  is in between 1.6 to 3.6 AU and  $\theta$  is in between 0 to  $2\pi$

Velocity: Chosen such that if Jupiter were absent, the asteroids would be in a circular orbit around the sun.

Number of asteroids: 1000

### 7.3 Plots

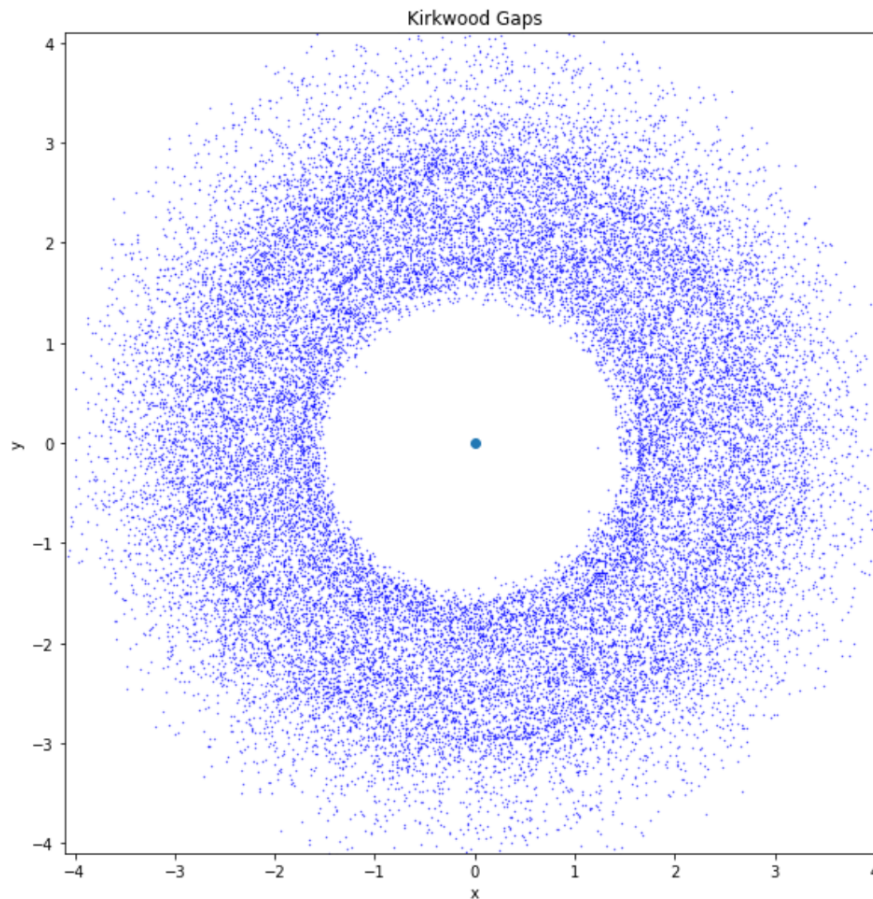


Figure 7.1: Kirkwood Gaps

### 7.4 Conclusion

More number of asteroids must be simulated to get Kirkwood gaps.